ACS APPLIED MATERIALS & INTERFACES

Letter

www.acsami.org

Quaternary Nanocomposites Consisting of Graphene, Fe_3O_4@Fe Core@Shell, and ZnO Nanoparticles: Synthesis and Excellent Electromagnetic Absorption Properties

Yu-Lan Ren,[†] Hong-Yu Wu,[†] Ming-Ming Lu,[‡] Yu-Jin Chen,*[,†] Chun-Ling Zhu,[§] Peng Gao,*[,§] Mao-Sheng Cao,[‡] Chun-Yan Li,[†] and Qiu-Yun Ouyang[†]

[†]College of Science and [§]College of Material Science and Chemical Engineering, Harbin Engineering University

[‡]School of Materials Science and Engineering, Beijing Institute of Technology, Beijing 100081, China

Supporting Information

ABSTRACT: This paper presents for the first time a successful synthesis of quaternary nanocomposites consisting of graphene, Fe_3O_4@Fe core/shell nanopariticles, and ZnO nanoparticles. Transmission electron microscopy measurements show that the diameter of the Fe_3O_4@Fe core/shell nanoparitcles is about 18 nm, the Fe_3O_4 shell's thickness is about 5 nm, and the diameter of ZnO nanoparticles is in range of 2−10 nm. The measured electromagnetic parameters show that the absorption bandwidth with reflection loss less than −20 dB is up to 7.3 GHz, and in the band range more than 99% of electromagnetic wave energy is attenuated. Moreover, the addition amount of the nanocomposites in the matrix is only 20 wt %. Therefore, the excellent electromagnetic absorption properties with lightweight and wide absorption frequency band are realized by the nanocomposites.

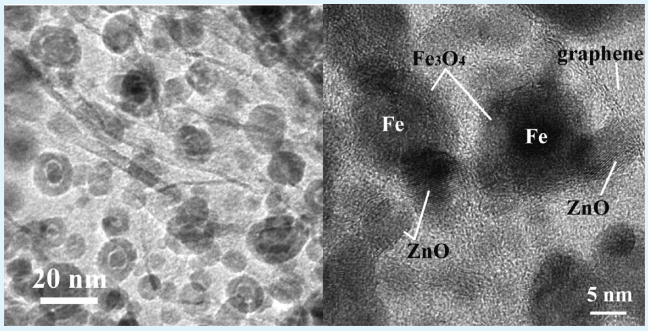

KEYWORDS: *graphene, Fe_3O_4, Fe, ZnO, quaternary nanocomposites, electromagnetic absorption*

INTRODUCTION

As a new class of two-dimensional carbon nanostructure, graphene (G) has attracted wide attention because of its excellent mechanical, electrical, thermal and optical properties.[1] Abundant chemical groups such as −OH and −C═O are introduced on its surface with a result that graphene can serve as an ideal substrate for the deposition of other functional materials. These functionalized graphenes exhibit new or enhanced physicochemical properties, and are promising for the applications in wide areas including energy storage and conversion,[2−18] chemical catalysts,[19−22] optoelectronic devices,[23−25] and sensors,[26] etc. Recently, exciting properties have been achieved by constructing the graphene-based ternary composites.[27−31] For example, reduced graphene oxide−porphyrin−ZnO, graphene−Fe_2O_3−polyaniline, and Pt−ITO−graphene ternary nanocomposites have been synthesized for the applications in photoconversion, photovoltaics, supercapacitors etc. Therefore, the construction of multi-functionalized graphene-based nanocomposites is very promising for their further applications.

Electromagnetic (EM) wave absorbing materials have attracted much attention due to the expanded EM interference problems. The traditional absorbers, such as ferrite, have strong absorption properties, but the thickness required is too large. Therefore, some kinds of nanomaterials, including magnetic metals, conducting polymer, and carbon nanotubes, have been studied for EM absorption.[32−35] However, the absorption property of such single material needs to be further improved. Recently, heteronanostructured materials with new or enhanced EM absorption properties have been reported.[36−44] For example, Ni/Ag core/shell nanoparticles showed dual-frequency EM absorption ability compared to the naked Ni particles;[36] polyaniline−multiwalled carbon nanotube nanocomposites could be used as both EM absorption and EM interface shielding materials;[37] the reflection loss reached −25 dB for carbon nanotube/Fe composites with a thickness of 1.2 mm.[38] Thus, good EM absorption property can be achieved by a reasonable construction of heteronanostructures.

Graphene has a very large surface area, resulting in its potential applications in lightweight EM absorbers. However, its high conductivity may degrade its EM absorption ability.[45] Although EM interface shielding properties of graphene and the ferromagnetic graphene composites have been investigated, their EM absorption properties have been seldom reported.[9,46,47] Herein, we design and synthesize new quaternary nanocomposites composed of graphene, Fe_3O_4@Fe core/shell nanoparticles, and ZnO nanoparticles as efficient and lightweight EM absorbing materials. Fe_3O_4@Fe core/shell nano-

Received: October 1, 2012
Accepted: November 23, 2012
Published: November 23, 2012

   dx.doi.org/10.1021/am3021697 | ACS Appl. Mater. Interfaces 2012, 4, 6436−6442

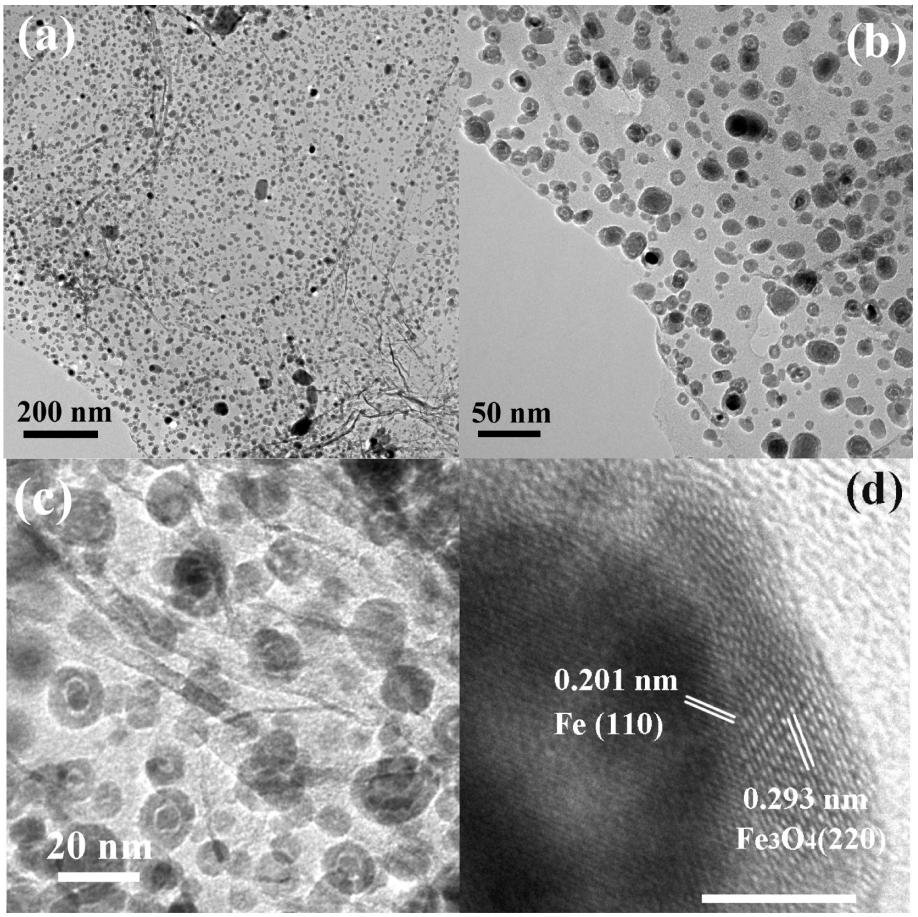

Figure 1. Structural characterizations of the G/Fe_3O_4@Fe ternary nanocomposites. (a) Low-resolution TEM image, (b, c) magnified TEM images, and (d) HRTEM image.

particles[48−52] and ZnO nanoparticles[35] are used as magnetic and dielectric loss materials, respectively. And the graphene serves as an ideal substrate for the deposition of the nanoparitcles. Because of their synergetic effect, interfacial polarization induced by multiple interfaces in the nanocomposites, and the charge−carrier transfer between Fe_3O_4 and ZnO, the quaternary nanoscomposites (G/Fe_3O_4@Fe/ZnO) exhibit excellent EM absorption performances.

EXPERIMENTAL SECTION

G/β−FeOOH nanohybrids were first synthesized, and ZnO nanoparticles were then deposited on them, forming G/β−FeOOH/ZnO nanocomposites. After the nanocomposites were annealed under an Ar/H_2 atmosphere, G/Fe_3O_4@Fe/ZnO quaternary nanoscomposites were successfully obtained. The detail synthesis process, structural characterization, and electromagnetic measurements were described in the Supporting Information (SI-1).

RESULTS AND DISCUSSION

Growth of β−FeOOH Nanocrystals on Graphene. Figure S1a (Supporting Information) shows a low-resolution TEM image of the as-synthesized G/β-FeOOH nanohybrids. It can be clearly seen that the β-FeOOH particles with a diameter less than 5 nm grow densely on the surface of graphene. Clear lattice fringes are observed in the high−resolution TEM (HRTEM) image (see Figure S1b in the Supporting Information), suggesting a crystal nature of the nanoparticles. Their selected area electron diffraction (SAED) pattern (see Figure S1c in the Supporting Information) shows diffraction rings, corresponding to (002), (200), (006), and (301) crystalline planes of orthorhombic β-FeOOH, respectively. The results above reveal that β-FeOOH nanocrystals have successfully grown on the surface of graphene by the present method.

Formation of G/Fe_3O_4@Fe Ternary Nanocomposites. β-FeOOH is transformed into Fe_3O_4 and α-Fe after the G/β-FeOOH nanohybrids are thermally treated at 420 °C for 5 h under Ar/H_2 flow, as shown in Figure S2a (Supporting Information). An additional small and broad diffraction peak appears at 2θ in range of 22.5−27.5° in the XRD pattern, which can be indexed to the disordered graphene sheets (Figure S2b, Supporting Information). Thus, the G/Fe_3O_4@Fe ternary nanocomposites have been synthesized through the above annealing process. It should be noted that iron oxides, such as γ−Fe_2O_3, may present in the product. Thus, X-ray photoelectron spectroscopy (XPS) measurements were carried out. Figure S3a (Supporting Information) shows the Fe 2p core level XPS spectra of the product. Two main peaks, located at 711.0 and 724.2 eV, correspond to Fe $2p_{3/2}$ and Fe $2p_{1/2}$, respectively. The signals are broadened, indicating that the Fe^{3+} and Fe^{2+} states coexist in the nanohybrids. Moreover, no shakeup satellite peaks, which are the fingerprints of the electronic structures of iron oxides such as α-Fe_2O_3 and γ-Fe_2O_3, can be identified. It indicates that Fe_2O_3 does not present in the nanohybrids.[53]

The morphologies and structures of the ternary nanocomposites were further investigated by TEM measurements.

dx.doi.org/10.1021/am3021697 | ACS Appl. Mater. Interfaces 2012, 4, 6436−6442

Figure 1a shows a low-resolution TEM image of the ternary nanocomposites. It can be clearly found that uniform nanoparticles with an average diameter of about 18 nm are deposited on the graphene's surface. Importantly, these nanoparticles disperse very well. Magnified TEM images (Figure 1b, c) show that the nanoparticles have very interesting structures, i.e., are composed of core and shell parts and the shell thickness is about 5 nm. Clearly lattice fringes are presented in both regions, as shown in Figure 1d, indicative of the crystal nature of the nanoparticles. However, the lattice spacings in the core and shell regions are significantly different. The spacing labeled in the core region is about 0.201 nm, corresponding to (110) plane of α-Fe, whereas it is about 0.293 nm in the shell region, corresponding to (220) plane of Fe_3O_4. Therefore, in terms of the TEM observations and the XRD and XPS analyses, we can draw a conclusion that β-FeOOH nanocrystals deposited on the graphene have been transformed into Fe_3O_4@Fe core/shell nanoparticles through the annealing process above, which has not been reported before.

Formation of G/Fe_3O_4@Fe/ZnO Quaternary Nanocomposites. The XRD analysis shows that Fe_3O_4, α-Fe, and ZnO are presented in the quaternary nanocomposites, as shown in Figure 2. The diffraction peaks of both graphene and

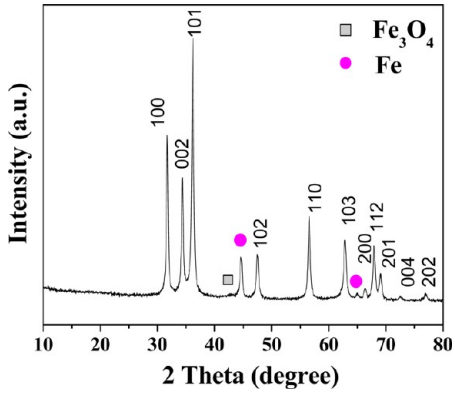

Figure 2. XRD pattern of the G/Fe_3O_4@Fe/ZnO quaternary nanocomposites.

Fe_3O_4 are suppressed because of strong diffraction intensities of ZnO. Similar to that of G/Fe_3O_4@Fe ternary nanocomposites, Fe_3O_4@Fe core/shell nanoparticles still cover over the surface of the graphene in the quaternary nanocomposites, as shown in Figure 3a. HRTEM image (Figure 3b) of an individual Fe_3O_4@Fe nanoparticle reveals that the core and shell materials are still α-Fe and Fe_3O_4, respectively. The possibility of other iron oxide phases is ruled out by the XPS analysis (Figure S3b). Besides Fe_3O_4@Fe core/shell nanoparticles, smaller nanoparticles with a size ranging from 2 to 10 nm are also clearly observed in the Figure 3a and Figure S4a (Supporting Information). According to XRD analysis the smaller nanoparticles should be ZnO. The presence of crystalline Fe_3O_4, α-Fe, and ZnO in the nanocomposites is also confirmed by the SAED pattern, as shown in Figure 3c. The diffraction rings in the pattern can be assigned to cubic Fe_3O_4 and body-centered cubic α-Fe, respectively, whereas the diffraction spots marked with white circles are due to hexagonal ZnO. Similar to the uniform distribution of Fe_3O_4@Fe core/shell nanoparticles, the ZnO nanoparticles also disperse well in the quaternary nanocomposites. The elemental distribution in the quaternary nanocomposites was further investigated by angular dark-field (ADF) STEM and energy-dispersive X-ray (EDX) element mapping analyses (see Figure S5 in the Supporting Information). The ADF STEM image and the EDX element mapping demonstrate that Fe, O and Zn elements are uniformly distributed in the nanocomposites. The ZnO nanoparticles are on the surface of graphene or on the surface or at the grain boundaries of Fe_3O_4@Fe core/shell nanoparticles, as shown in Figure 3a. Thus, four kinds of material interfaces, i.e., G−ZnO, G−Fe_3O_4, Fe_3O_4−Fe, and Fe_3O_4−ZnO, are presented in the unique quaternary nanoscomposites. Figure 3d shows a magnified TEM image of the quaternary nanocomposites. The locations of graphene, Fe_3O_4, α-Fe, and ZnO are marked with white lines. HRTEM images of ZnO nanoparticles marked with the white and black frames in the Figure 3d are shown in the upper left and lower left insets of Figure 3c, respectively. The lattice spacings are 0.262 ± 0.004 nm, corresponding to (002) plane of hexagonal ZnO. The TEM image also shows that parts of ZnO nanoparticles are bonded with both graphene and Fe_3O_4@Fe core/shell nanoparticles, and thus graphene−Fe_3O_4−ZnO triple junctions also form in the quaternary nanocomposites. The content of graphene in the quaternary nanocomposites is determined by the energy dispersive spectroscopy (EDS) analysis, as shown in Figure S4b (Supporting Information). The molar ratio of C to Fe, Zn, and O is about 1.5:1:0.3:1.

Magnetic Properties of the Ternary and Quaternary Nanocomposites. The field dependence of magnetization for the ternary and quaternary nanocomposites was measured at room temperature by a vibrating sample magnetometer, as shown in Figure 4. Significant hysteresis loops in the $M-H$ curves indicate the ferromagnetic behavior of both the ternary nanocomposites and the quaternary nanocomposites. The saturation magnetization (M_s), coercivity (H_c), and retentivity (M_r) are 98.5 emu/g, 235.9 Oe, and 11.6 emu/g respectively for the ternary nanocomposites, and 13.8 emu/g, 197.8 Oe, and 3.3 emu/g respectively for the quaternary nanocmposites. The magnetic measurements above demonstrate that the nanocomposites are ferromagnetic, suggesting that they may be used to attenuate EM irradiation because of multidomain walls in the Fe_3O_4 nanoparticles.[48−52]

The analyses above reveal that multi-interfaces and triple junctions exist in the ferromagnetic G/Fe_3O_4@Fe/ZnO quaternary nanocomposites, which would have important effect on their EM absorption properties. The addition amount of the nanocomposites into the paraffin matrix is 20 wt % for the investigation of the EM absorption properties as detailed below.

EM Absorption Properties. According to the previous report, graphene had weak ability of EM attenuation.[9] In contrasts, the G/Fe_3O_4@Fe ternary nanocomposites and the G/Fe_3O_4@Fe/ZnO quaternary nanocomposites exhibited significantly improved EM absorption properties. The measured EM parameters (the relative complex permittivity: $\varepsilon_r = \varepsilon' - j\varepsilon''$, and the relative complex permeability: $\mu_r = \mu' - j\mu''$) show that the ternary and quaternary nanocomposites have relatively larger both dielectric loss and magnetic loss compared with other magnetic materials (see Figures S6 and S7 in the Supporting Information), suggesting that they have good EM absorption properties.[48−52] According to the transmission line theory,[54] reflection loss (R_L) can be calculated by the following equations

$$Z_{in} = (\mu_r/\varepsilon_r)^{1/2}\tanh[j2\pi fd/c)(\mu_r\varepsilon_r)^{1/2}] \quad (1)$$

dx.doi.org/10.1021/am3021697 | ACS Appl. Mater. Interfaces 2012, 4, 6436−6442

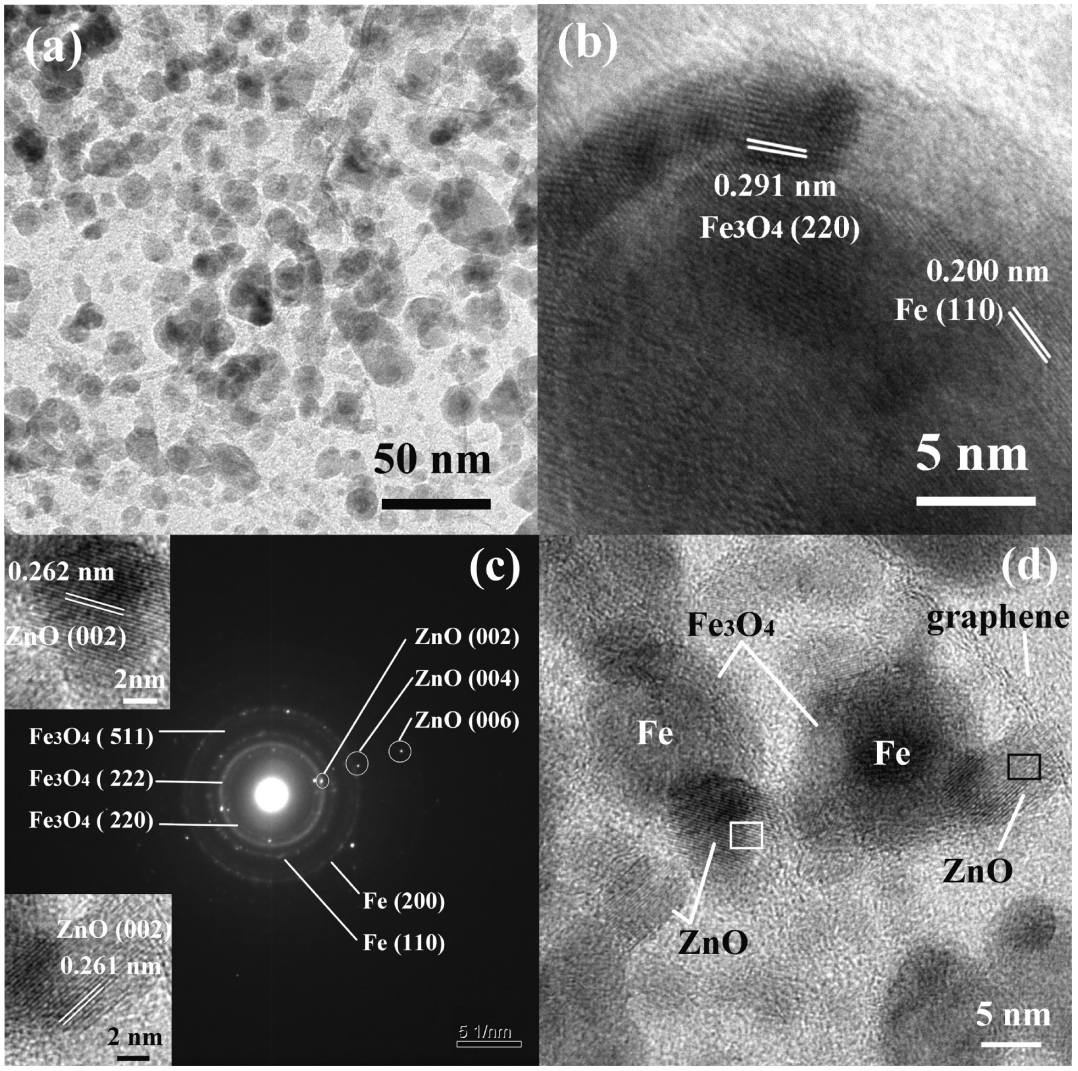

Figure 3. Structural characterizations of the G/Fe_3O_4@Fe/ZnO quaternary nanocomposites. (a) Low-resolution TEM image, (b) HRTEM image of an individual Fe_3O_4@Fe nanoparticle in the nanocomposites, (c) SAED pattern, and (d) HRTEM image for the triple junctions. The upper and lower insets show HRTEM images of ZnO nanoparticles marked with white and black frames in d, respectively.

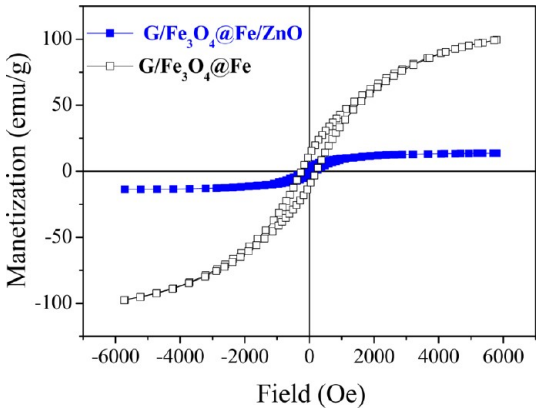

Figure 4. Magnetization hysteresis loops measured at room temperatures. (a) G/Fe_3O_4@Fe ternary nanocomposites and (b) the G/Fe_3O_4@Fe/ZnO quaternary nanocomposites.

$$R_L(\mathrm{dB}) = 20\log\left|\frac{Z_{in} - 1}{Z_{in} + 1}\right| \quad (2)$$

where Z_{in} is the input impedance of the absorber, c is the velocity of electromagnetic waves in free space, f is the frequency of microwaves, and d is the thickness of the absorber. The calculated reflection losses (R_L) of the ternary nanocomposites are shown in Figure 5a. It can be found that the minimal R_L values are less than −17 B for the nanocomposites with the thicknesses in the range of 2−5 mm. However, all of the values for the graphene are larger than −11 dB.[9] The detail comparisons of the R_L values between the G/Fe_3O_4@Fe ternary nanocomposites and the graphene are listed in Table1. Therefore the ternary nanocomposites exhibit greatly enhanced EM absorption properties in comparison with the graphene. After the deposition of ZnO nanoparticles on the ternary nanocomposites, their EM absorption properties are further improved, as shown in Figure 5b. It can be found that the minimal R_L values are less than −30 dB for the nanocomposites with the thicknesses 2.5−5 mm. Importantly, the absorption bandwidth with R_L less than −20 dB is up to 7.3 GHz (in the frequency range of 5.9−15.2 GHz). Because more than 99% of EM wave energy can be attenuated by the absorber when its R_L value is less than −20 dB, the G/Fe_3O_4@Fe/ZnO quaternary nanocomposites show excellent EM absorption properties.

dx.doi.org/10.1021/am3021697 | ACS Appl. Mater. Interfaces 2012, 4, 6436−6442

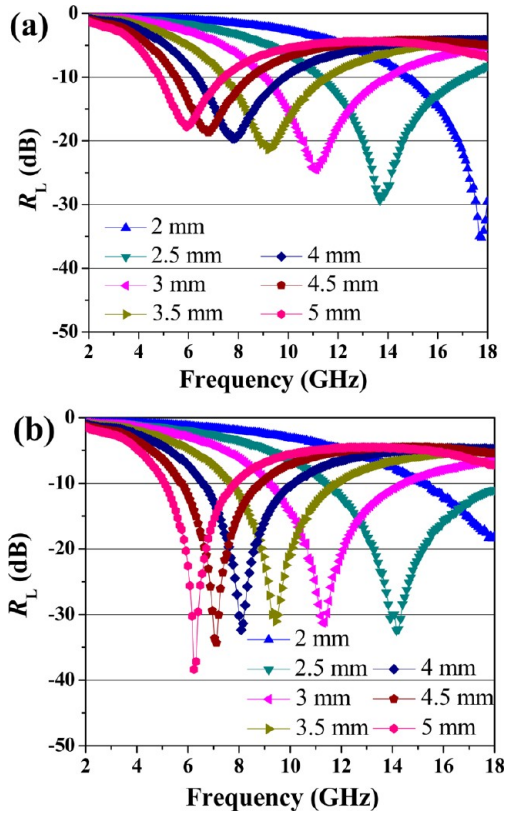

Figure 5. Reflection losses of the (a) G/Fe_3O_4@Fe ternary nanocomposites and (b) G/Fe_3O_4@Fe/ZnO quaternary nanocomposites with thickness 2−5 mm.

Considering edge effect (the calculated reflection losses in frequency ranging from 4 to 16 GHz are more reliable[38]) the absorption band for the ternary nanocomposites is only about 3.5 GHz (from 8.8 to 14.6 GHz). The detailed comparison of the R_L values between the ternary and quaternary nanocomposites is also summarized in Table 1. In addition, the reflection losses for G/ZnO nanocomposites with the thicknesses in the range of 2−5 mm are larger than −20 dB, as shown in Figure S8 in the Supporting Information. Therefore, the G/Fe_3O_4@Fe/ZnO quaternary nanocomposites have better EM absorption properties in comparison with the ternary nanocomposites, G/ZnO nanocomposites and the graphene.

In addition, compared with other magnetic materials such as Fe_3O_4/TiO_2, Fe_3O_4/carbo,n and Fe_3O_4/SnO_2 core/shell nanostructures, G/Fe_3O_4@Fe/ZnO quaternary nanocomposites exhibit very good EM absorption properties.[48,51,52] For example, the R_L values of the Fe_3O_4/TiO_2 core/shell nanotubes are larger than −20.6 dB as the thickness is in range of 2−5 mm. Moreover, the added weight of these magnetic materials in the matrix is more than 40 wt %. Thus, the G/Fe_3O_4@Fe/ZnO quaternary nanocomposites can be used as lightweight EM absorbing materials with good absorption properties.

As pointed out above, the multi-interfaces and triple junctions are presented in the G/Fe_3O_4@Fe/ZnO quaternary nanocomposites. The enhanced Debye relaxation process induced by the interfaces has also contributed to the improved EM absorption properties. According to the Cole−Cole dispersion laws, the Debye relaxation process is able to be reflected in the plot of $\varepsilon' - \varepsilon''$. In the plot, each semicircle corresponds to one Debye relaxation process.[9] The plots for the quaternary and ternary nanocomposites (Figure S9, Supporting Information) show that the quaternary nanocomposites have one semicircle more than the ternary nanocomposites, indicating that the interface polarization plays an import role in the enhanced EM properties. In general, the excellent EM wave absorptions are strongly dependent on the efficient complementarities between dielectric and magnetic losses, that is, if dielectric tangent loss ($\tan \delta_e = \varepsilon''/\varepsilon'$) is equal to the magnetic tangent loss ($\tan \delta_m = \mu''/\mu'$), the absorber will show the best EM absorption property. Only magnetic loss or only dielectric loss leads to poor EM absorption properties.[40,48] The relationships between $\tan \delta_e$ and $\tan \delta_m$ show that the complementarities of the quaternary nanocomposites are better than those of the ternary nanocomposites especially in low-frequency region (Figure S10, Supporting Information). In addition, the Fe 2p spectrum in the G/Fe_3O_4@Fe/ZnO quaternary nanocomposites shifts about 0.2 eV lower in binding energy compared to that of the G/Fe_3O_4@Fe ternary nanocomposites. It reveals that the surrounding ZnO nanoparticles have important effect on the electric structures of Fe_3O_4 and the charge-carrier transfer between Fe_3O_4 and ZnO would occur as an external field is applied,[55] which contributes to the enhanced EM absorption properties.

CONCLUSION

The G/Fe_3O_4@Fe/ZnO quaternary nanocomposites have been synthesized, in which Fe_3O_4@Fe core/shell nanoparticles and ZnO nanoparticles are uniformly deposited on the graphene. The multi-interfaces and triple junctions are presented in the quaternary nanocomposites, which results in their significantly enhanced EM absorption properties. The minimal R_L values are less than −30 dB for the quaternary nanocomposites with the thicknesses 2.5−5 mm and the absorption bandwidth with the R_L values less than −20 dB is up to 7.3 GHz. It indicates that more than 99% of EM wave energy is attenuated by the nanocomposites. Moreover, the addition amount of the nanocomposites in the matrix is only 20 wt %. Therefore, G/Fe_3O_4@Fe/ZnO quaternary nanocomposites are very promising for the applications in lightweight EM absorbing materials. The enhanced EM absorption mechanism is also discussed, which is attributed to the enhanced Debye relaxation process in terms of the Cole−Cole dispersion laws, the complementarities between dielectric and magnetic losses of the quaternary nanocomposites, and the charge-carrier transfer between Fe_3O_4 and ZnO. Our results demonstrate that the excellent EM absorption properties with lightweight and wide absorption

Table 1. Detail Comparison of the R_L Values among the Ternary and Quaternary Nanocomposites and the Graphene

d (mm)	2	2.5	3	3.5	4	4.5	5	
R_L, min (dB)	−11.0	−9.4	−8.0	−7.0	−6.1	−6.2	−6.4	graphene
R_L, min (dB)	−35.2	−29.3	−24.5	−21.4	−19.7	−18.7	−17.8	G/Fe_3O_4@Fe
R_L, min (dB)	−18.4	−32.5	−31.3	−31.1	−32.4	−34.3	−38.4	G/Fe_3O_4@Fe/ZnO

dx.doi.org/10.1021/am3021697 | ACS Appl. Mater. Interfaces 2012, 4, 6436−6442

frequency band are realized by constructing the graphene-based nanocomposites.

■ ASSOCIATED CONTENT

Supporting Information

Experimental details, structural characterizations of G/β-FeOOH nanohybrids, XPS spectra, the EM parameters, the Cole−Cole semicircles, and the tangent losses of the G/Fe_3O_4@Fe ternary nanocomposites and the G/Fe_3O_4@Fe/ZnO quaternary nanocomposites, STEM, elemental mapping, SEM image and EDS pattern of the G/Fe_3O_4@Fe/ZnO quaternary nanocomposites, XRD pattern of the G/Fe_3O_4@Fe ternary nanocomposites, and the reflection losses of the G/ZnO nanocomposites. This material is available free of charge via the Internet at http://pubs.acs.org/.

■ AUTHOR INFORMATION

Corresponding Author

*E-mail: chenyujin@hrbeu.edu.cn (Y.-J.C.); gaopeng@mail.neu.edu.cn (G. P.).

Notes

The authors declare no competing financial interest.

■ ACKNOWLEDGMENTS

We thank the National Natural Science Foundation of China (Grants 51072038, 51272050, 61205113, 51172275, and 21001035), Program for New Century Excellent Talents in University (NECT−10−0049), and Outstanding Youth Foundation of Heilongjiang Province (Grant JC201008) for the financial support of this research.

■ REFERENCES

(1) Novoselov, K. S.; Geim, A. K.; Morozov, S. V.; Jiang, D.; Zhang, Y.; Dubonos, S. V.; Grigorieva, I. V.; Firsov, A. *Science* **2004**, *306*, 666−669.
(2) Wang, H. L.; Casalongue, H. S.; Liang, Y. Y.; Dai, H. J. *J. Am. Chem. Soc.* **2010**, *132*, 7472−7477.
(3) Wang, H. L.; Cui, L. F.; Yang, Y.; Casalongue, H. S.; Robinson, J. T.; Liang, Y. Y.; Cui, Y.; Dai, H. J. *J. Am. Chem. Soc.* **2010**, *132*, 13978−13980.
(4) Wu, Z. S.; Ren, W. S.; Wen, L.; Gao, L. B.; Zhao, J. P.; Chen, Z. P.; Zhou, G. M.; Li, F.; Cheng, H. M. *ACS Nano* **2010**, *4*, 3187−3194.
(5) Zhou, G. M.; Wang, D. W.; Li, F.; Zhang, L. L.; Li, N.; Wu, Z. S.; Wen, L.; Lu, G. Q.; Cheng, H. M. *Chem. Mater.* **2010**, *22*, 5306−5313.
(6) Xu, Z.; Gao, C. *Nat. Commun.* **2011**, *2*, 571.
(7) He, H. K.; Gao, C. *ACS Appl. Mater. Interfaces* **2010**, *2*, 3201−3210.
(8) Chen, Y. J.; Wang, Q. S.; Zhu, C. L.; Gao, P.; Ouyang, Q. Y.; Wang, T. S.; Ma, Y.; Sun, C. W. *J. Mater. Chem.* **2012**, *22*, 5924−5927.
(9) Yu, H. L.; Wang, T. S.; Wen, B.; Lu, M. M.; Xu, Z.; Zhu, C. L.; Chen, Y. J.; Xue, X. Y.; Sun, C. W.; Cao, M. S. *J. Mater. Chem.* **2012**, *22*, 21679−21685.
(10) Yang, H. B.; Guo, C. X.; Guai, G. H.; Song, Q. L.; Jiang, S. P.; Li, C. M. *ACS Appl. Mater. Interfaces* **2011**, *3*, 1940−1945.
(11) Chen, D. Y.; Ji, G.; Ma, Y.; Lee, J. Y.; Lu, J. M. *ACS Appl. Mater. Interfaces* **2011**, *3*, 3078−3083.
(12) Chen, S.; Zhu, J. W.; Wu, X. D.; Han, Q. F.; Wang, X. *ACS Nano* **2010**, *4*, 2822−2830.
(13) Biswas, S.; Dral, L. T. *Chem. Mater.* **2010**, *22*, 5667−5671.
(14) Chang, K.; Chen, W. X.; Ma, L.; Li, H.; Li, H.; Huang, F. H.; Xu, Z. D.; Zhang, Q. B.; Lee, J. Y. *J. Mater. Chem.* **2011**, *21*, 6251−6257.
(15) Chang, K.; Chen, W. X. *ACS Nano* **2011**, *5*, 4720−4728.
(16) Sun, Y. M.; Hu, X. L.; Lou, W.; Huang, Y. H. *ACS Nano* **2011**, *5*, 7100−7107.
(17) Yang, S. B.; Feng, X. L.; Mullen, K. *Adv. Mater.* **2011**, *23*, 3575−3579.
(18) Zhang, Y. J.; Mori, T.; Niu, L.; Ye, J. H. *Energy Environ. Sci.* **2011**, *4*, 4517−4521.
(19) Xu, C.; Wang, X.; Zhu, J. W. *J. Phys. Chem. C* **2008**, *112*, 19841−19845.
(20) Li, Y. G.; Wang, H. L.; Xie, L. M.; Liang, Y. Y.; Hong, G. S.; Dai, H. J. *J. Am. Chem. Soc.* **2011**, *133*, 7296−7299.
(21) Williams, G.; Seger, B.; Kamat, P. V. *ACS Nano* **2008**, *2*, 1487−1491.
(22) Jin, Z.; Nackashi, D.; Lu, W.; Kittrell, C.; Tour, J. M. *Chem. Mater.* **2010**, *22*, 5695−5699.
(23) Cao, A. N.; Liu, Z.; Chu, S. S.; Wu, M. H.; Ye, Z. M.; Cai, Z. W.; Chang, Y. L.; Wang, S. F.; Gong, Q. H.; Li, Y. F. *Adv. Mater.* **2010**, *22*, 103−106.
(24) Ji, Y. S.; Lee, S. C.; Cho, B.; Song, S. H.; Lee, T. *ACS Nano* **2011**, *5*, 5995−6000.
(25) Wang, Y.; Zhen, S. J.; Zhang, Y.; Li, Y. F.; Huang, C. Z. *J. Phys. Chem. C* **2011**, *115*, 12815−12821.
(26) Rangel, N.; Gimenez, A.; Sinitskii, A.; Seminario, J. M. *J. Phys. Chem. C* **2011**, *115*, 12128−12134.
(27) Hayashi, H.; Lightcap, I. V.; Tsujimoto, M.; Takano, M.; Umeyama, T.; Kamat, P. V.; Imahori, H. *J. Am. Chem. Soc.* **2011**, *133*, 7684−7687.
(28) Xia, X. F.; Hao, Q. L.; Lei, W.; Wang, W. J.; Sun, D. P.; Wang, X. *J. Mater. Chem.* **2012**, *22*, 16844−16850.
(29) Kou, R.; Shao, Y. Y.; Mei, D. H.; Nie, Z. M.; Wang, D. H.; Wang, C. M.; Viswanathan, V. V.; Park, S.; Aksay, I. A.; Lin, Y. H.; Wang, Y.; Liu, J. *J. Am. Chem. Soc.* **2011**, *133*, 2541−2547.
(30) Min, Q. H.; Zhang, X. X.; Zhang, H. Y.; Zhou, F.; Zhu, J. J. *Chem. Commun.* **2011**, *47*, 11709−11711.
(31) Xia, X. F.; Hao, Q. L.; Lei, W.; Wang, W. J.; Wang, H. L.; Wang, X. *J. Mater. Chem.* **2012**, *22*, 8314−8320.
(32) Watts, P. C. P.; Hsu, W. K.; Barnes, A.; Chambers, B. *Adv. Mater.* **2003**, *15*, 600−603.
(33) Wadhawan, A.; Garrett, D.; Perez, J. M. *Appl. Phys. Lett.* **2003**, *83*, 2683−2685.
(34) Deng, L. J.; Han, M. *Appl. Phys. Lett.* **2007**, *91*, 023119.
(35) Chen, Y. J.; Cao, M. S.; Wang, T. H.; Wan, Q. *Appl. Phys. Lett.* **2004**, *84*, 3367−3369.
(36) Lee, C. C.; Chen, C. H. *Appl. Phys. Lett.* **2007**, *90*, 193102.
(37) Saini, P.; Choudhary, V.; Singh, B. P.; Mathur, R. B.; Dhawan, S. K. *Mater. Chem. Phys.* **2009**, *113*, 919−926.
(38) Che, R. C.; Peng, L. M.; Duan, X. F.; Chen, Q.; Liang, X. L. *Adv. Mater.* **2004**, *16*, 401−405.
(39) Saini, P.; Arora, M. Microwave Absorption and EMI Shielding Behavior of Nanocomposites Based on Intrinsically Conducting Polymers, Graphene and Carbon Nanotubes. In *New Polymers for Special Applications*; Gomes, A. D., Ed.; InTech: Rijeka, Croatia, **2012**; DOI: 10.5772/48779.
(40) Che, R. C.; Zhi, C. Y.; Liang, C. Y.; Zhou, X. G. *Appl. Phys. Lett.* **2006**, *88*, 033105.
(41) Li, N. L.; Huang, Y.; Du, F.; He, X. B.; Lin, X.; Gao, H. J.; Ma, Y. F.; Li, F. F.; Chen, Y. S.; Eklund, P. C. *Nano Lett.* **2006**, *6*, 1141−1145.
(42) Zhang, X. F.; Dong, X. L.; Huang, H.; Liu, Y. Y.; Wang, W. N.; Zhu, X. G.; Lv, B.; Lei, J. P.; Lee, C. G. *Appl. Phys. Lett.* **2006**, *89*, 053115.
(43) Zhu, J. H.; Wei, S. Y.; Haldolaarachchige, N.; Young, D. P.; Guo, Z. H. *J. Phys. Chem. C* **2011**, *115*, 15304−15310.
(44) Zhu, J. H.; Wei, S. Y.; Zhang, L.; Mao, Y. B.; Ryu, J.; Haldolaarachchige, N.; Young, D. P.; Guo, Z. H. *J. Mater. Chem.* **2011**, *21*, 3952−3959.
(45) Wang, C.; Han, X. J.; Xu, P.; Zhang, X. L.; Du, Y. C.; Hu, S. R.; Wang, J. Y.; Wang, X. H. *Appl. Phys. Lett.* **2011**, *98*, 072906.
(46) Liang, J. J.; Wang, Y.; Huang, Y.; Ma, Y. F.; Liu, Z. F.; Cai, J. M.; Zhang, C. D.; Gao, H. J.; Chen, Y. S. *Carbon* **2009**, *47*, 922−925.
(47) Tung, T. T.; Feller, J. F.; Kim, T.; Kim, H.; Yang, W. S.; Suh, K. S. *J. Polym. Sci., Part A: Polym. Chem.* **2012**, *50*, 927−935.

(48) Chen, Y. J.; Gao, P.; Wang, R. X.; Zhu, C. L.; Wang, L. J.; Cao, M. S.; Jin, H. B. *J. Phys. Chem. C* **2009**, *113*, 10061−10064.
(49) Chen, Y. J.; Cao, M. S.; Wang, T. H.; Wan, Q. *J. Appl. Phys.* **2009**, *106*, 054303.
(50) Chen, Y. J.; Zhang, F.; Zhao, G. G.; Fang, X. Y.; Jin, H. B.; Gao, P.; Zhu, C. L.; Cao, M. S.; Xiao, G. *J. Phys. Chem. C* **2010**, *114*, 9239−9244.
(51) Zhu, C. L.; Zhang, M. L.; Qiao, Y. J.; Xiao, G.; Zhang, F.; Chen, Y. J. *J. Phys. Chem. C* **2010**, *114*, 16229−16235.
(52) Chen, Y. J.; Xiao, G.; Wang, T. S.; Ouyang, Q. Y.; Qi, L. H.; Ma, Y.; Gao, P.; Zhu, C. L.; Cao, M. S.; Jin, H. B. *J. Phys. Chem. C* **2011**, *115*, 13603−13608.
(53) Fujii, T.; de Groot, F. M. F.; Sawatzky, G. A.; Voogt, F. C.; Hibma, T.; Okada, K. *Phys. Rev. B* **1999**, *59*, 3195−3202.
(54) Kim, S. S.; Jo, S. B.; Choi, K. K.; Kim, J. M.; Churn, K. S. *IEEE Trans. Magn.* **1991**, *27*, 5462−5464.
(55) Tseng, R. J.; Baker, C. Q.; Shedd, B.; Huang, J. X. *Appl. Phys. Lett.* **2007**, *90*, 053101.